Available online at www.sciencedirect.com
SCIENCE DIRECT®
Thermochimica Acta 413 (2004) 39–46
thermochimica acta
www.elsevier.com/locate/tca

Analysis of thermally stimulated current and effect of rubbery annealing around glass-rubber transition temperature in polyethylene terephthalate

N. Benrekaa [a,b,*], A. Gourari [a], M. Bendaoud [a], K. Ait-hamouda [b]

[a] *Université des Sciences et Technologies Houari Boumedienne BP. 32, El Alia, 16111 Bab Ezzouar, Algiers, Algeria*
[b] *Unité de Développement de la technologie du Silicium UDTS 2, Bd Frantz Fanon, BP. 399 Algiers, Algeria*

Received 19 March 2003; received in revised form 20 October 2003; accepted 20 October 2003

Abstract

Thermally stimulated currents (TSC) in amorphous polyethylene terephthalate films have been investigated in the temperature range of −180 to 140 °C. This material shows a very weak intensity peak at approximately −95 °C and another around 80 °C originated from dipolar process (α-peak), as evidenced from the variation of polarizing conditions such as applied electric field and polarizing time. The effect of isochronal rubbery annealing starts to appear from a temperature of annealing of 90 °C, it then appears in a TSC spectrum two components around 88 and 108 °C allotted, respectively to the true and rigid amorphous phases. The first component tends to disappear in an irreversible way to the detriment of the second which implies the establishment of an order within material during annealing by the formation and growth of nodules. The thermostimulated currents technique allowed to calculate with good precision the activation parameters of each process as well as the evaluation of the crystallinity rate by an established empirical formula.

Keywords: Thermally stimulated currents (TSC); PET; Rubbery annealing

1. Introduction

The thermally stimulated currents (TSC) technique has been widely used to study fundamental characteristics in various materials including films, powders, bulk specimen, crystalline and amorphous insulators. TSC measurements were made to identify the origin of the molecular relaxations and allows detection and resolution of transitions that other techniques cannot see or separate [1–7].

TSC technique consists of applying a dc voltage to a material in order to orient dipoles sensitive to electric field [8]. The temperature is then lowered (with the field maintained) in order to reduce internal motion, by this fact trapping the polarized dipole within the material. The electric field is then switched off and the sample reheated, allowing thermal energy to release the "trapped" molecular motions. As this occurs, a small current is observed, corresponding to one or more types of relaxation. This technique provides advantages in both sensitivity and sample preparation. The output is a plot of depolarization current versus temperature, showing global peaks for each motion taking place during the recovery process. Temperature can be scanned from −180 to 400 °C, exploring the rubber and rubbery flow region as easily as the solid state. The output is very similar to a plot of tan δ versus T obtained with (DMA) [7] at very low frequencies, but with higher sensitivity.

In amorphous polyethylene terephthalate sample, it is generally accepted that above room temperature TSC spectrum exhibits two main relaxation peaks, the first one localized around 80–90 °C, i.e., in the range of the glass-rubber transition temperature T_g and the second one above 120 °C whose position and exact nature are subject of controversy in literature [9–12]. At low temperature, a weak amplitude peak is localized at about −95°C and extends over a large domain [−175 and −20 °C].

The aim of this work is to analyze the nature of TSC spectrum in amorphous PET in the temperature range from liquid nitrogen temperature to above T_g, effects of thermal heating and polarization conditions.

Thermal windowing technique (thermal sampling or peak cleaning method) [13], was applied to study individual modes of relaxation for the two main peaks, i.e., around glass-rubber transition α-peak and at lowest temperature

* Corresponding author. Fax: +213-21-24-7344.
E-mail address: bnas@voila.fr (N. Benrekaa).

0040-6031/$ – see front matter © 2003 Elsevier B.V. All rights reserved.
doi:10.1016/j.tca.2003.10.026

β-peak. The specific relaxation parameters have been determined using different methods including the initial rise method of Gasanly et al. [14] or Williams et al. [15] expressions for the relaxation time, the integration of the peak and the fitting of experimental data with the analytical expression of the current.

Polyethylene terephthalate has been selected as the material of choice. It has the advantage of being studied either in the purely amorphous state or in partially crystalline state at different degrees of crystallinity and crystal perfection [16]. The results will be interpreted in terms of simple phenomenological models.

2. Experimental

2.1. Experiment part

The measurements were carried out on polyethylene terephthalate PET samples, supplied by Dupont de Nemours (Luxembourg) in 55 μm thickness and used in form of square sheets (1.2 cm^2). The samples were vacuum evaporated with 100 nm thickness aluminum electrodes and 1 cm diameter to opposite sides and had been previously polished using polishing rouge and dry methanol. Evaporated electrodes were used to prevent an air gap being trapped between the electrode and the sample and to increase ohmic contact [17]. The sample with electrodes shorted is located in measurement chamber which was maintained at a constant and desired pressure of 10^{-3} mbar with inert N_2 gas. The glass transition temperature of 75 °C was determined by differential scanning calorimetry [18]. The DSC measurements were performed in a Perkin–Elmer DSC7 differential scanning calorimeter with a controlled cooling accessory. The temperature of the instrument was calibrated with indium and lead standards and only the same indium sample was used for the heat flow calibration. The calibration were performed during heating at 10 °C/min. The sample was placed in a sealed aluminum cupel. The mass of PET fragments must have a maximum contact area between the sample and the cupel. A mass higher than 5 mg proved to be acceptable. The recording of the spectra of DSC transition was carried out for heating rates about 10 °C/min.

By keeping the sample at 130 °C for hours or even days, the crystallinity attains its maximum value and remains unchanged during the experimental period. Thus, in order to avoid the crystallinity of amorphous PET during classical TSC procedures, the upper measurement temperature must not exceed 95 °C.

The current was measured with an electrometer (Keithley 614) and recorded by using *X–Y* plotter. A platinum temperature sensor PT100, mounted in the sample holder and adjacent to the film, allowed the temperature measurement with a precision of 0.25 °C. The heating rate of 8 °C/min was used and controlled by a temperature regulator (BT 300/302 CLTS).

The complex TSC spectrum was obtained by submitting the sample to an constant electrical field $E_p = 10^6$ V/m during 2 min at a temperature of polarization $T_p = 75$ °C. The sample is then cooled with a ramp of 8 °C/min to liquid nitrogen temperature in the presence of the electrical field. The field is then suppressed at around −175 °C and the electrodes were short-circuited for 15 min, and then the sample was heated at 8 °C/min to 140 °C. All measurements were repeated to verify the reproducibility and the accuracy of the results.

2.2. Basic considerations for peaks analysis

In general, the built-up of polarization at a constant temperature T can be described by the equation [19]

$$P(t) = P_0\left[1 - \exp\left(-\frac{t}{\tau}\right)\right] \tag{1}$$

where τ and P_0 are respectively, the relaxation time of dipoles and the maximum amount of polarization possible at temperature T with,

$$P_0 = \left(\frac{N\mu^2 E_p}{3k_B T}\right) \tag{2}$$

where N is the concentration of dipoles, E_p the local electric field and μ the dipole moment which is independent of temperature, k_B Boltzman's constant.

We may represent the temperature variation of the relaxation time τ by the Arrehinus type equation [19]

$$\tau(T) = \tau_0 \exp\left(\frac{w}{k_B T}\right) \tag{3}$$

where τ_0^{-1} is the characteristic frequency factor for a vacancy jump from a lattice site to another for orientation of the dipoles and is independent of temperature and w the activation energy.

The current density released during a thermally stimulated measurement can be expressed [19]

$$J'(T) = -\frac{N\mu^2 E_p}{\tau_0 3k_B T}\exp - \left(-\frac{w}{k_B T} + \frac{1}{\beta\tau_0}\int_{T_0}^{T}\exp\left(-\frac{w}{k_B T}\right)\mathrm{d}T'\right) \tag{4}$$

where $\beta = \mathrm{d}T/\mathrm{d}t$ is the heating rate.

$$\text{By introducing} \quad J'(T) = \frac{P_0 J(T)}{P(T)} \tag{5}$$

$$\text{We obtain} \quad J'(T) = \text{constant} - \left(\frac{w}{k_B T}\right) \tag{6}$$

The plot of $\ln(J')$ as function of $1/k_B T$ is a straight line, whose slope gives the value of w and $\ln(\tau_0)$.

For the determination of the characteristic parameters of the process, i.e., the activation energy and the pre-exponential factor, the initial rise method is mostly used.

The integral in Eq. (4) can be approximated as an asymptotic expansion [19]

$$\ln J(T) = \ln A - \frac{w}{k_B T} - \frac{B}{\beta}\int_{T_0}^{T} \exp\left(\frac{-w}{k_B T'}\right) \mathrm{d}T' \tag{7}$$

where

$$A = \frac{P_0}{\tau_0}; \quad B = \frac{1}{\tau_0} \tag{8}$$

by introducing

$$I = \int_{T_0}^{T} \exp\left(\frac{-w}{k_B T}\right) \mathrm{d}T \cong \left\{ TE_2\left(\frac{w}{k_B T}\right) - T_0 E_0\left(\frac{w}{k_B T_0}\right)\right\} \tag{9}$$

where $E_n(z)$ is the integral exponential function [20] given by

$$E_n(z) = \int_1^{\infty} \frac{\mathrm{e}^{-zt}}{t^n}\mathrm{d}t, \quad \mathrm{Re}(z) > 0 \tag{10}$$

we obtain

$$\ln j(T) \cong \ln A - f - \frac{BT}{\beta f}\left(1 - \frac{2}{f} + \frac{6}{f^2} - \cdots\right)\exp(-f) \tag{11}$$

with

$$f = \frac{w}{k_B T} \quad (\text{for } T < T_g) \text{ or } f = \frac{w}{k_B(T - T_\infty)} \quad (\text{for } T > T_g)$$

The use of Eq. (11) presents an advantage of using more experimental points particularly in the region where the current reaches its maximum. From the values obtained for A, w and B from the fitting, the characteristic parameters of the process may be determined.

The relaxation time associated with an elementary peak may be deduced from

$$\tau(T) = \frac{P(T)}{J(T)} \tag{12}$$

3. Results

Fig. 1 presents the differential scanning calorimetry (DSC) measurement on amorphous PET sample, it shows a broad and a weak glass-rubber transition around 75 °C (the thermogram shows the glass transition as a step in the specific heat capacity, covering a temperature interval from 60 to 80 °C. The glass transition temperature, defined as the temperature of the midpoint of the rise of heat capacity in the transition, is 75 °C), and melting at about 260 °C. Around 130 °C an exothermic peak is observed corresponding to the crystallization. The thermogram was recorded by using Perkin–Elmer DSC7 calorimeter.

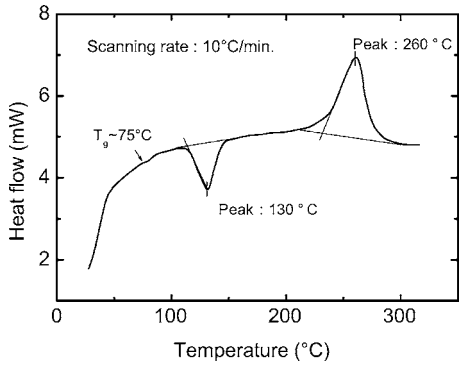

Fig. 1. DSC spectrum of amorphous polyethylene terephthalate film as received. (Scanning rate 10 °C/min, PET mass used 8 mg).

3.1. α and β relaxation modes

In Fig. 2 the complex spectrum was obtained by polarizing to $T_p = 75$ °C during 2 min (time enough long for reaching the equilibrium polarization) by a static electric field $E_p = 10^6$ V/m. The sample was then quenched to −175 °C using liquid nitrogen which enables orientation polarization $P(T_p)$ to be frozen-in and the field was cut off.

The complex spectrum reveals two quite distinct peaks at the positions $T_{M1} = -95$ °C and $T_{M2} = 78$ °C related respectively to β and α relaxations [21–23].

A polarization at 0 °C by the electric field $E_p = 10^6$ V/m and a short circuit at −175 °C allow the isolation of the peak represented on the Fig. 3, this latter is named β peak related to β relaxation [24]. The maximum of the current is localized around −95 °C and the peak extends from −175 to −20 °C.

To study in details this relaxation mode, the β relaxation peak has been experimentally resolved into a set of elementary spectra with the peak cleaning method and a thermal window of 10 °C as shown in inset graph of Fig. 3.

Each of these elementary relaxation curves can be mathematically transformed into their Arrhenius representation and plotted as ln(τ) versus $1/T$ which express the variation

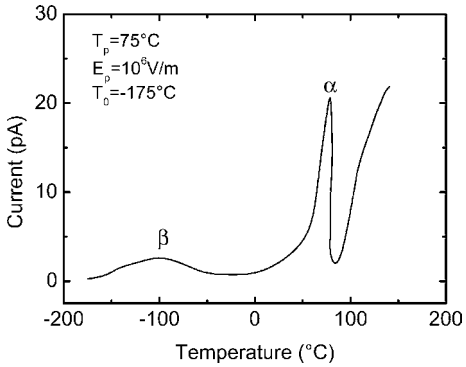

Fig. 2. TSC spectrum scanned from −175 to 140 °C in inert N_2 gas for a well conditioned amorphous PET sample. Polarization field 10^6 V/m, heating rate 8 °C/min, polarization temperature 75 °C.

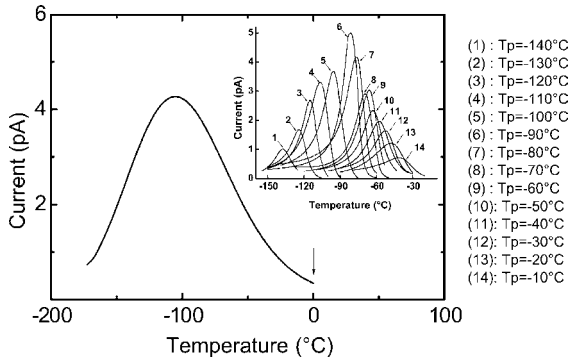

Fig. 3. TSC peak profile for amorphous PET sample obtained by thermal windowing technique (inset of plot: polarization window $\Delta T = 10\,^{\circ}\mathrm{C}$, T_p varies from -140 to $-10\,^{\circ}\mathrm{C}$, polarization field 10^6 V/m, heating rate $8\,^{\circ}\mathrm{C}$/min) and complex spectra in the β range, the arrow indicates the initial polarization temperature.

of the relaxation time versus temperature as shown in the individual lines (Fig. 4).

The activation energy and τ_0 were calculated assuming a dipolar origin using Bucci–Fieschi–Guidi method (Eq. (3)).

The initial rise method was used as well and the results are reported in Table 1.

At about 80 °C, the asymmetric and intensive α peak was also isolated with $T_p = 75\,^{\circ}\mathrm{C}$ and $T_0 = 0\,^{\circ}\mathrm{C}$ and resolved into a set of elementary peaks with $\Delta T = 5\,^{\circ}\mathrm{C}$ (Fig. 5).

On this figure the appearance of distribution around 80 °C is noted. The envelope of the elementary peaks reproduces qualitatively the shape of the main peak. The transformation of all elementary peaks obtained with thermal windowing method (peak cleaning method) into their Arrhenius representation (Fig. 6) allow the correlation between single relaxation modes and thermokinetic (free energy, entropy, and enthalpy) and/or other physical variables [25,26] (Table 2).

A particular attention was given to this peak because of its amplitude, thermal position and its response to the polarization conditions.

Table 1
The specific parameters, for β relaxation process involved in the release of the current, determined by the use of initial rise method (IR), and the peak integration method (BFG)

T_{Pl} (°C)	ΔH (eV) IR	ΔH (eV) BFG	τ_0(s)
−140	0.23	0.31	1.39×10^{-10}
−130	0.27	0.36	3.53×10^{-12}
−120	0.20	0.39	0.90×10^{-12}
−110	0.35	0.42	6.34×10^{-12}
−100	0.37	0.44	3.33×10^{-12}
−90	0.38	0.47	2.63×10^{-12}
−80	0.39	0.51	4.12×10^{-15}
−70	0.40	0.56	7.20×10^{-16}
−60	0.43	0.65	2.39×10^{-18}
−50	0.45	0.72	4.52×10^{-18}
−40	0.47	0.77	0.97×10^{-19}
−30	0.51	0.79	0.88×10^{-19}
−20	0.56	0.83	0.69×10^{-19}
−10	0.62	0.91	6.78×10^{-20}

PET sample was polarized from -140 to $-10\,^{\circ}\mathrm{C}$ with polarization window of $10\,^{\circ}\mathrm{C}$, heating rate $10\,^{\circ}\mathrm{C}$/min and $E_p = 10^6$ V/m in inert N_2 gas.

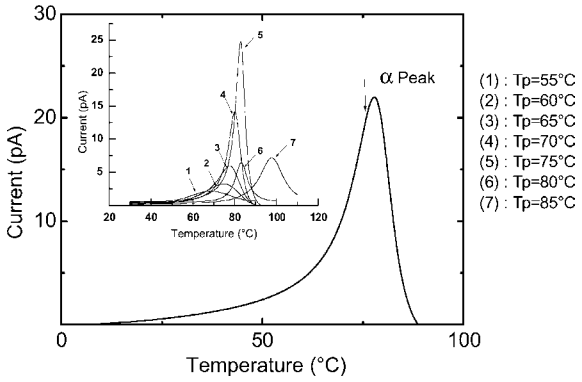

Fig. 5. TSC peak profile for amorphous PET sample obtained by thermal windowing technique (inset of plot: polarization window $\Delta T = 5\,^{\circ}\mathrm{C}$, T_p varies from 55 to 85 °C, polarization field 10^6 V/m, heating rate $8\,^{\circ}\mathrm{C}$/min) and complex spectra in the α range, the arrow indicates the initial polarization temperature.

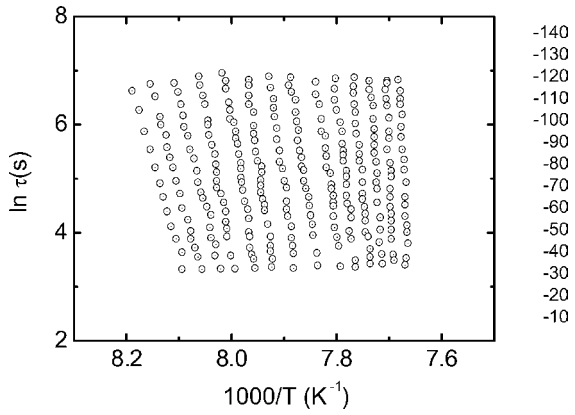

Fig. 4. Arrhenius plot of the relaxation times obtained from TSC measurement. The right hand numbers are the polarization temperatures (T_p). Each line corresponds to a certain T_p.

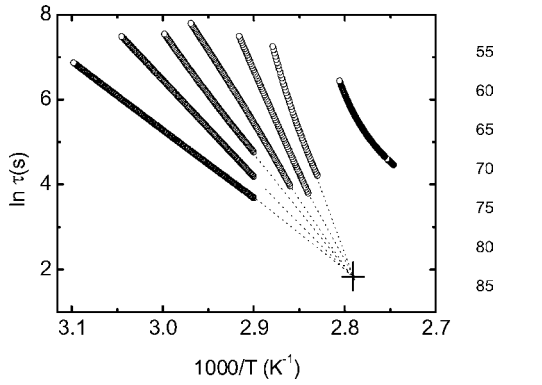

Fig. 6. Arrhenius plot of the relaxation times obtained from TSC measurement for α peak. The right hand numbers are the polarization temperature T_p. Dashed lines are fits according to the Arrhenius equation. The graph shows a positive compensation around ($T = 86.6\,^{\circ}\mathrm{C}$, $\tau = 28.9$ s).

Table 2
The specific parameters, for α relaxation process involved in the release of the current, determined by the use of the peak integration method and fitting of experimental data

T_P (°C)	T_{max} (°C)	ΔH (eV) (BFG)	ΔH (eV) (curve fit)	τ_0(s)
55	69.56	1.08	0.98	2.24×10^{-14}
60	75.20	1.51	1.47	1.79×10^{-20}
65	78.49	1.91	1.83	3.51×10^{-26}
70	81.22	2.29	2.01	1.32×10^{-31}
75	82.25	3.02	2.69	1.04×10^{-41}
80	82.72	4.89	4.05	1.00×10^{-67}

PET sample was polarized from 55 to 80 °C with polarization window of 5 °C, heating rate 8 °C/min and $E_p = 10^6$ V/m in inert N_2 gas.

3.2. Influence of polarization conditions on α peak

Fig. 7 shows the behavior of the α peak as a function of the polarizing time t_p at 75 °C and at a constant polarizing voltage V_p. The inset graph displays a significant dependence of α peak magnitude on t_p. Besides, the α peak originating from a dipolar process may not reach a near-saturation level of polarization at a polarizing time $t_p < 10$ min.

A linear dependence of the α peak value on the polarizing field may be observed in Fig. 8, and expected with dipolar processes. Concerning the temperature position of the peaks maximums, it does not seem affected by the electric field and remains constant (≈78 °C).

3.3. Study of rubbery annealing effect

To carry out a rubbery annealing on initially amorphous PET, we heat the sample from room temperature T_r until a temperature T_a definitely higher than the glass transition temperature T_g. In this temperature range ($T > T_g$), the material is in a state known as rubbery. As soon as the temperature is stabilized at T_a we maintain this state during an interval of time $\Delta t_a = 20$ min which corresponds to the duration of rubbery annealing, that we can vary at will. The result of such process on the initially amorphous material is mainly obtaining a semi-crystalline PET. This procedure is called "cold" crystallization [27] because the ordered structure obtained results from the glass state. Within our framework, we carried out annealing on six samples cut out from the same film. On each one, we carried out isochronal annealing at various temperatures T_a (Table 3).

The complex spectra obtained for each sample are reported on Fig. 9. It is important to note that the same conditions of polarization have been maintained for each recording i.e., the same electric field $E_p = 10^6$ V/m and the same polarization temperature $T_p = 80$ °C.

The recorded spectra reveal a segregation of a relaxation mode around 100 °C. This thermal manifestation is due primarily to simultaneous presence of two phases: a completely

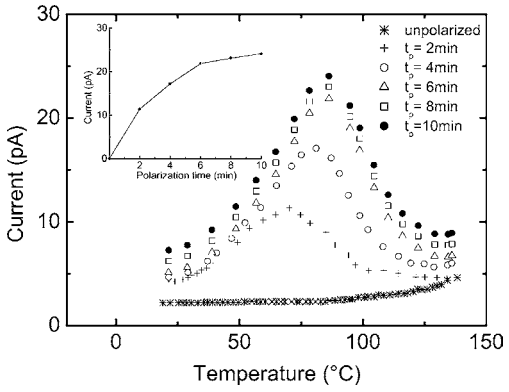

Fig. 7. TSC spectra of PET film (thickness 55 μm) corresponding to different times of polarization t_p. Temperature of polarization $T_p = 75$ °C. Polarizing voltage $V_p = 30$ V, heating rate 8 °C/min. The dependence of the α-peak value on the polarization time is shown in the inset.

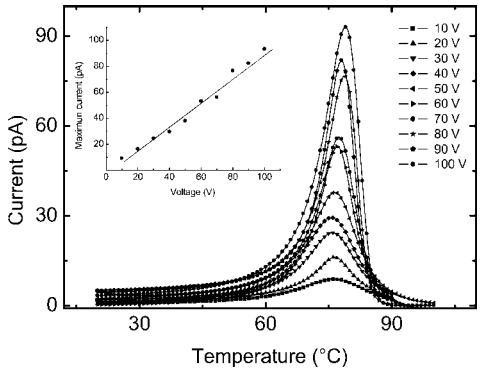

Fig. 8. TSC spectra of PET film (thickness 55 μm) for different polarization voltages (10–100 V with an increment of 10 V), heating rate 8 °C/min, polarization temperature 75 °C. Dependence of the α-peak value on polarization voltage is shown in the inset.

Table 3
Temperatures of annealing of the various samples, $t_r = 20$ min (T_a varies from 90 to 140 °C with an increment of 10 °C)

Sample	PET_1	PET_2	PET_3	PET_4	PET_5	PET_6
T_a (°C)	90	100	110	120	130	140

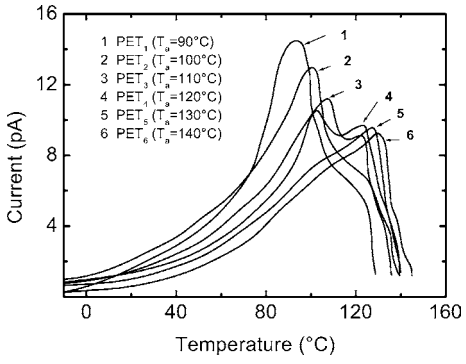

Fig. 9. Effect of isochronal annealing at different temperature T_a on the main relaxation peak (α) (T_a varies from 90 to 140 °C with an increment of 10 °C). Polarization temperature $T_p = 80$ °C, heating rate 8 °C/min, $E_p = 10^6$ V/m.

amorphous phase indicated by "true" amorphous phase and a semi-crystalline phase. For a rubbery annealing at 90 °C the first phase appears by a significant amplitude peak around 88 °C followed by a shouldering in the vicinity of 108 °C due to semi-crystalline phase manifestation.

As the temperature of isothermal annealing T_a increases, a reduction of the peak intensity related to the amorphous phase is observed and emergence of a second peak corresponding to the semi-crystalline phase. For an annealing at 130 °C we observe almost a disappearance of the first peak which is reduced to a simple shoulder around 99.4 °C and a considerable intensity increase of the second peak.

4. Discussion

The α relaxation mode observed at $T_{max} = 80$ °C (main relaxation mode) is attributed to glass transition manifestation. This latter is clearly detected in all amorphous polymers. Significant atoms movements of the main chain are associated to this transition. Disordered movements animate the amorphous segments [28,29].

The elementary peaks exploitation of the α mode allows to plot $\ln(\tau) = f(1000/T)$ diagrams according to Arrhenius equation.

The value 3.02 eV of the activation enthalpy, in the vicinity of the glass transition characterizes a main relaxation mode [23].

The existence of a compensation phenomenon [26,30–32] is observed for the α relaxation mode. Indeed, from the Arrhenius diagram (Fig. 6) it was observed that all the lines converge towards a point. Its coordinates give the parameters ($T_c = 86.61$ °C, $\tau_c = 28.94$ s) representing, respectively the temperature and time compensations. Moreover, the linear evolution of $\ln(\tau)$ versus ΔH confirms the existence of such phenomenon characterizing the mobile amorphous phase. This phenomenon is associated to the existence of an order in the amorphous phase of the material [30].

The last elementary peak isolated at $T_{max} = 98.7$ °C presents a different behavior than those isolated at lower temperatures. In fact Arrhenius shows a nonlinear variation. This later was resolved using the Vögel equation

$$\tau(T) = \tau_{0V} \exp\left[\frac{1}{\alpha_f (T - T_\infty)}\right] \quad (13)$$

T_∞ determination allows a linearization of $\ln(\tau) = f(1000/T - T_\infty)$. The value of $T_\infty = 25$ °C seems the best. α_f and τ_{0v} parameters are reported on Table 4. The value $T_{gWLF} = 76.6$ °C, deduced from Williams, Landel and Ferry equation ($T_{gWLF} = T_\infty + 51.6$ °C) accords well with the glass transition temperature value $T_g = 75$ °C, characterizing the amorphous PET. Besides, the value of the free volume dilatation coefficient ($\alpha_f = 1.43 \times 10^{-3}$ °C^{-1}) is near to WLF empiric value [15].

Table 4
Vögel parameters related to the peak isolated at $T_{max} = 98.7$ °C with: $T_p = 85$ °C, heating rate of 8 °C and polarization field $E_p = 10^6$ V/m

T_p (°C)	T_{max} (°C)	T_∞ (°C)	T_{gWLF} (°C)	τ_{0v}(s)	α_f (°C^{-1})
85	98.7	25	76.6	2.44×10^{-3}	1.43×10^{-3}

The polarization electric field influence is manifested by the increase of the main peak current amplitude by a linear way, confirming the dipolar relaxations process.

This increase is explained by the fact that the electric field E_p affects more dipoles as when its intensity increases.

The low temperatures relaxation mode (mode β) is very broad and less intense compared to the main peak $I^{\alpha}_{max}/I^{\beta}_{max} = 7.6$. The calculated activation energy by the initial rise method is always lower than that determined by the Bucci–Fieschi–Guidi method. Furthermore, the dielectric β relaxation for this material has an activation energy of 0.58 eV. For good known amorphous polymers as the PS, the PMMA, the PET ..., the activation energy of the β relaxation is about 0.6 eV [19,23]. In addition the formation enthalpy of a quasi-punctual defect ΔH_F is about $3k_BT_g$ approximately 0.1 eV. Under these conditions, we conceive that, even if the structural unit implied in the β relaxation process is arranged in the most compact possible way with its neighbors, the thermal fluctuation of energy can cause the movement via the formation of a defect. In other words, the activation energy of the β relaxation is generally equalized with

$$E_\beta = E_m + \Delta H_F \quad (\Delta H_F < E_m), \quad (14)$$

where E_m is the height of the energy barrier to cross at the time of the movement; E_m includes an intermolecular component but probably, an intramolecular component. In this case, the structural determinant parameter should be the density of left conformations: it is important to note that the experimental data do not allow the establishment of a clear and final relation between this density (in other words, the rigidity of the chain) and the intensity of β relaxation; nevertheless let us mention that it is precisely in the case of two amorphous polymers with rigid chains (PC and PEEK) that a difficulty appears to identify in a sure way the β relaxation.

As the temperature of rubbery annealing increases, the material acquires more and more crystallinity, which appears in a TSC spectrum by a segregation of mode.

The first mode observed on TSC spectra relates to the real amorphous phase, always present in material. The second mode appears starting from a temperature of annealing $T_a = 110$ °C relates to the semi-crystalline phase.

The real amorphous phase tends to disappear partially to the detriment of the semicrystalline phase in the same direction of the increase of T_a. This later is due to the formation of crystallites within material. However, in the case of a rubbery annealing carried out from the ambient temperature T_r until a temperature T_a ($T_g < T_a <$

Table 5
Arrhenius parameters and rate of crystallinity for various temperatures of isochronal annealing ($\Delta t_a = 20$ min)

T_a (°C)	ΔH (eV)	τ_0(s)T_g	T_c (°C)	χ(TSC)
90	3.52	3.11×10^{-39}	81.63	5.76
100	3.09	6.02×10^{-37}	81.82	5.94
110	2.87	5.54×10^{-31}	85.84	9.97
120	2.43	1.91×10^{-27}	87.91	12.04
130	2.36	2.59×10^{-26}	91.22	15.35
140	2.11	7.22×10^{-24}	94.82	18.95

100 °C) the crystalline phase originates from the crystallite formation of new nodules in the material, when $T_a > 100$ °C the crystallites grow without formation of new nodules.

The rubbery annealing effect of on PET moves the temperature of the maximum of each relaxation mode to high temperatures. Decomposition in elementary spectra allowed to plot Arrhenius diagrams of the six samples to assess the activation energies of each process and the rate of crystallinity (Table 5).

Arrhenius diagrams obtained usually shows a compensation phenomenon at compensation temperatures T_{ci} (i relates to each annealing temperature). Knowing this compensation temperature besides the glass transition temperature T_g permit to obtain the rate of crystallinity in the material from empiric formula we have deducted

$$\chi \equiv T_c - \gamma \left[\frac{T_g^2(\mathrm{DSC})}{T_g(\mathrm{TSC})} \right], \quad (15)$$

where γ is a correction factor (for PET $\gamma \approx 0.98$).

T_g(DSC) and T_g(TSC) are the glass transition temperatures determined by DSC and TSC, respectively.

The results obtained are summarized in Table 5.

The activation enthalpy decreases when the annealing temperature increase, it is supposed that this fact is due to the decrease of the relaxing entities dimensions and numbers when the crystallinity increase.

5. Conclusion

Thermal relaxation behavior of amorphous PET have been investigated over a wide range of temperature by thermally stimulated current technique. TSC measurement performed on well conditioned samples reveals the existence of two dipolar relaxation modes around glass-rubber transition temperature and at −95 °C. The enthalpy determination from Arrhenius plots is around 3.02 eV in the case of the dominant α relaxation mode and about 0.6 eV for the secondary β relaxation mode. The method has been applied to determine the influence of rubbery annealing on changes of material structure appear in a TSC spectrum by a mode segregation, confirming a simultaneous presence of both amorphous and semi-crystalline phases. Using compensation parameters from Arrhenius plots of the relaxation times for the annealed samples, an empirical formula was established to reach a quick evaluation of the crystallinity rate.

Acknowledgements

The authors would like to express their gratitude to M.R. Oudih of Algiers Nuclear Research Center CRNA and C. Guerbi of Silicon Technology Development Unit UDTS for technical discussions and S. Benrekaa for assistance.

References

[1] O.M. Bordurn, Phys. Stat. Sol. (a) 176 (1999) 1089.
[2] A. Gourari, Ph.D thesis, University of Sciences and Technologies, Algiers, 1995.
[3] G.M. Venkatesh, M.E. Barnett, C. Owusu-Fordjour, M. Galop, Pharma. Res. 18 (2001) 98.
[4] I. Pintilie, D. Petre, L. Pintilie, C. Tivarus, M. Petris, T. Botila, Nucl. Instrum. Meth. A 439 (2000) 303.
[5] A. Gourari, M. Bendaoud, J. Chim. Phys. 90 (1993) 2007.
[6] A. Gourari, M. Bendaoud, C. Lacabanne, R. Boyer, J. Poly. Sci. Phys. 23 (1985) 889.
[7] J.R. Saffel, A. Matthiesen, R. McIntyre, J.P. Ibar, Thermochim. Acta 192 (1991) 243.
[8] J. Van Turnhout, Thermally Stimulated Discharge of Polymer Electrets, Elsevier, Amsterdam, 1975.
[9] M.M. Perlman, R.A. Creswell, J. Appl. Phys. 42 (1971) 531.
[10] Yu. Gorokhovatsky, D. Temnov, J.N. Marat-Mendes, J.M. Dias, D.K. Das Gupta, J. Appl. Phys. 83 (1998) 5337.
[11] E.R. Neagu, P. Pissis, J.N. Marat-Mendes, J.L. Gomez Ribelles, R.M. Neagu, in: Proceedings of the Ninth International Symposium on Electrets, Shanghaï, China, 1996.
[12] A. Maeda, K. Kojima, Y. Takai, M. Idea, Jpn. J. Appl. Phys. 23 (1984) 1260.
[13] S. Devautour, J. Vanderschuren, J.C. Guitini, F. Henn, J.V. Zanchetta, J. Appl. Phys. 82 (1997) 5057.
[14] N.M. Gasanly, A. Aydinli, Ö. Salihoglu, Cryst. Res. Technol. 36 (2001) 295.
[15] M.L. Williams, R.F. Landel, J.D. Ferry, J. Am. Chem. Soc. 77 (1955) 370.
[16] R.J. Seyler, Thermal Anal. 49 (1997) 491.
[17] Kwang-Suck Suh, IEEE Electr. Insul. 8 (1992) 13.
[18] P.G. Royall, D.Q.M. Craig, C. Doherty, Pharma. Res. 15 (1998) 1117.
[19] E. Neagu, J.N. Marat-Mendes, D.K. Das-Gupta, R.M. Neagu, R. Igreja, J. Appl. Phys. 82 (1997) 2488.
[20] M. Abramowitz, I.A. Stegun, Handbook of Mathematical Functions, Dover Publication Inc., New York, 1970.
[21] G.F. Leal Ferreira, M.T. Figueiredo, S.N. Fedosov, J.A. Giacometti, J. Phys. D Appl. Phys. 31 (1998) 2051.
[22] E. Neagu, P. Pissis, L. Apekis, J.L. Gomez Ribelles, J. Phys. D Appl. Phys. 30 (1997) 1551.
[23] Jo. Perez Physique et Mécanique des Polymères Amorphes, Tech. Doc. Lavoisier Publication, 1992.
[24] E. Dargent, M. Kattan, J. Grenet, C. Cabot, in: Proceedings of the 10th International Symposium on Electrets, 1999.
[25] J.P. Ibar, in: Proceedings of ANTEC'88 Conference, Atlanta, 1988.
[26] J.P. Ibar., in: Proceedings of NATAS Symposium, Cambridge, 1990.

[27] M.T. Connor, M.C. Garcia Gutiérrez, D.R. Rueda, F.J. Balta Calleja, J. Mater. Sci. 32 (1997) 5615.
[28] R.F. Boyer, Encyclopedia of Polymer Science, Wiley, New York, 1977.
[29] N. Benrekaa, A. Gourari, in: Proceedings of the International Congress of Science and Material Engenieering, ICMSE'99, USTHB Algiers, 1999.
[30] C.J. Dias, J.N. Marat-Mendes, in: Proceedings of the 10th International Symposium on Electrets, 1999.
[31] G. Teyssèdre, C. Lacabanne, J. Phys. D Appl. Phys. 28 (1995) 1478.
[32] J.D. Hoffmann, G. Williams, E. Passaglia, J. Polym. Sci. 14 (1966) 173.